

## Master-slave synchronization in chaotic discrete-time oscillators

J. Schwarz,<sup>1,2,\*</sup> A. Klotz,<sup>1</sup> K. Bräuer,<sup>1</sup> and A. Stevens<sup>2</sup>

<sup>1</sup>*Institut für Theoretische Physik, Universität Tübingen, Morgenstelle 14, D-72076 Tübingen, Germany*

<sup>2</sup>*Universitätsklinik für Psychiatrie und Psychotherapie, Oslanderstrasse 24, D-72076 Tübingen, Germany*

(Received 15 June 2000; revised manuscript received 21 March 2001; published 20 June 2001)

In this paper, we study a simple discrete-time neural oscillator model that, in certain parameter regimes, exhibits periodic or chaotic dynamics. The present model with intrinsically chaotic dynamics is capable of spatiotemporal information processing: in response to constant external stimulation, the oscillator can switch into different chaotic states restricted to distinct parts of the phase space. Of particular interest is the processing of time-dependent input in a master-slave configuration of two coupled oscillators. Here, the response of an oscillator is studied by driving it with the signal of the other. Following the input, the response system adapts to the state of the drive. For a chaotic drive, we can observe generalized synchronization. The onset of adaptation to the drive state by the response is accompanied by on-off intermittency resulting in irregular bursting behavior.

DOI: 10.1103/PhysRevE.64.011108

PACS number(s): 05.10.-a, 84.35.+i

### I. INTRODUCTION

Chaotic dynamics is a frequent phenomenon even in simple neural network models, but it has been thought of as being of no direct computational relevance. Computation with chaotic neural networks attracted much interest after the observation that chaotic dynamics may be directly involved in the neurocomputational activities of the brain [1]. There are several approaches concerning computation with chaotic neural networks. Such networks may allow us to realize associative memories with enormous storage capacity, since an infinite number of unstable periodic orbits (UPOs) is embedded in a chaotic attractor, each of which can be stabilized using chaos control techniques [2]. Chaotic dynamics can also be used during the network's learning cycle to prevent the network from becoming captured in undesired local minima [3]. Furthermore, chaotic neural networks can learn correlations between time series, which can be applied to prediction and modeling of sequence generation [4]. In addition, neural networks with chaotic attractors are expected to allow a more biologically realistic approach to perform computational tasks: such systems encode and classify stimuli by altering their dynamics rather than by converging to a static pattern.

To illustrate this, one may consider the well-known Lorenz attractor. Recognition of an input pattern may stabilize the network dynamics onto individual parts of the attractor, e.g., onto one of the two wings of the Lorenz attractor. There is ample evidence for the validity of this suggestion from several experimental studies as well as mathematical models of the olfactory bulb [5]. It is believed that in the absence of signals from olfactory receptors, the activity of the olfactory bulb is chaotic and of low amplitude. Signals from the receptors reduce the dimension of the attractor, or even make the chaotic activity coherent and periodic.

Coupled nonlinear oscillators allow us to investigate the

functional role of coherent activity in the brain. Synchrony generation by networks of interconnected neurons has been the subject of many theoretical and numerical studies [6]. Synchronization can manifest itself in different ways. The common meaning of synchronization is the coincidence of events or motions with respect to time. As a basic phenomenon in physics and biology, synchronization refers to the simultaneous occurrence of entrainment (1:1 frequency locking) and phase locking in weakly coupled oscillator ensembles. Following widespread study of chaotic oscillators, the notion of synchronization has been generalized to these systems [7,8]. Coupled identical deterministic chaotic systems can synchronize perfectly: once the coupling exceeds a critical value, both systems move along identical orbits. A method to study synchronization in chaotic systems was proposed by Pecora and Carroll [7]. They split a chaotic system into two subsystems, a drive and a response system. They find that drive and response will typically synchronize only if the maximal Lyapunov exponent of the response subsystem is negative. In general, such a situation can be studied by equations of the form

$$\begin{aligned}\dot{u}(t) &= F(u(t), v(t)), \\ \dot{v}(t) &= G(v(t)).\end{aligned}\tag{1}$$

Since the coupling is active only in one direction, such a system is referred to as a master-slave system with slave  $U$  and master  $V$  and with state variables  $u = \{u_1, \dots, u_r\}$  and  $v = \{v_1, \dots, v_d\}$ .

If the coupled systems are not identical, in general they cannot move along identical orbits. But if they are both chaotic and noise-free, a measurable interdependency can still exist, provided the coupling is sufficiently strong [9]. This is referred to as generalized synchronization, which in nonidentical chaotic systems of the form (1) can be obtained if a relation  $u(t) = \Psi(v(t))$  exists. Identical synchronization requires  $\Psi = \mathbf{1}$ , whereas the condition for generalized synchronization is less restrictive. As suggested by Pyragas [10],  $\Psi$  can be either a smooth transformation, where the generalized

---

\*Corresponding author. Email address: juergen.schwarz@uni-tuebingen.de

synchronization is strong, or a nowhere continuous transformation  $\Psi$ , where the generalized synchronization is weak. In general, it is not possible to construct  $\Psi$  explicitly, and even if it were, it would not be clear to what extent deviations from predicted values are due to a lack of synchronization or to an inexactness of  $\Psi$ . When the exact equations of motion are known, generalized synchronization can be inferred from the Lyapunov exponents of Eqs. (1) or from the identical synchronization of two identical slave systems. New measures of generalized synchronization suitable for experimental data have been proposed recently [11].

In biology, both ways of coupling—reciprocal and master-slave—coexist. As an example, cortex and thalamus as structures are reciprocally connected; they are not, however, on the cellular scale. For example, thalamic input is fed into layer IV neurons, but cortico-thalamic projection originates in layer VI cortical neurons. Within the cortex, pyramidal cells and interneurons are partly reciprocally connected, partly not, and form functional compartments within the cortex. Other examples of master-slave configurations are found in the cortico-striatal projection, in the cerebellar circuitry, in the hippocampal-lateral-medial septum pathway, or the entorhinal-nucleus accumbens pathway.

The mechanisms of inducing synchronous firing in groups of cells are not yet accessible to experimental study, since too many “parameters” are impossible or at least difficult to control by means of pharmacological techniques. When excitable systems are subject to an external stimulus, the question arises under which conditions they can be entrained. A pair of neurons could be synchronized either via direct synaptic connection between them or as a result of a common input.

In this work, we study two coupled chaotic discrete-time neural oscillators based on a model proposed by Wang [12]. The intrinsic dynamics of these oscillators and their response to constant external stimuli are well understood. However, an understanding of the dynamic properties of coupled, small ensembles is also essential, especially in view of larger networks. A description of the model and its basic properties are presented in Sec. II. In Secs. III and IV, we present a numerical study of the dynamics of a master-slave system and we show the dependence of the systems behavior on the parameter master-slave coupling strength and constant external input on the drive system. The overall behavior of the slave system in response to the resulting chaotic drive is analyzed by calculating bifurcation diagrams. The synchronization properties of the master-slave system are determined by explicitly calculating the maximal Lyapunov exponent assigned to the slave system. Section V gives a summary of the results and a general discussion of the neurocomputational and neurobiological properties of the model.

## II. MATHEMATICAL DESCRIPTION

### A. A discrete-time neural oscillator model

Most works on neural oscillators focus on continuous-time models, such as, for instance, the Wilson-Cowan model [13]. Discrete-time models received relatively little attention, though their behavior often differs fundamentally from their

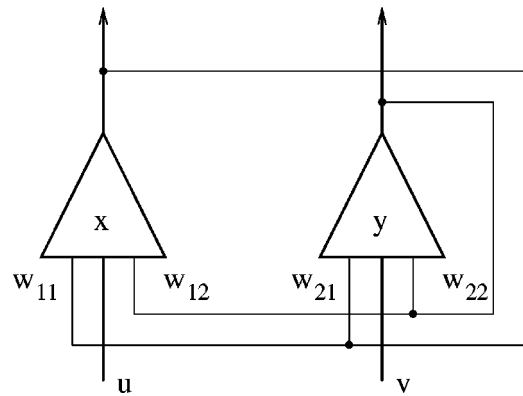


FIG. 1. Schema of the discrete-time oscillator  $(x,y)$  with synaptic weights  $w_{ij}$  and external inputs  $u$  and  $v$ .

continuous-time counterparts. Even simple discrete-time oscillators can produce a variety of dynamical behavior ranging from fixed points through quasiperiodicity to chaos. A general discrete-time neural oscillator model is given by

$$\begin{aligned} x^{t+1} &= f(w_{xx}x^t + w_{xy}y^t + u + \theta_x), \\ y^{t+1} &= f(w_{yx}x^t + w_{yy}y^t + v + \theta_y), \end{aligned} \quad (2)$$

where  $x$  and  $y$  are the state variables of a pair of an excitatory and an inhibitory neuron, the  $w_{ij}$  are the synaptic weights,  $\theta_i$  are fixed thresholds, and  $u$  and  $v$  are external inputs. A schematic representation of Eqs. (2) is shown in Fig. 1. The output function  $f$  is given by a sigmoidal function, such as  $f(z) = \tanh(\mu z)$  or the Fermi function

$$f(z) = \frac{1}{1 + e^{-4\sigma z}}. \quad (3)$$

For the intrinsic dynamics of Eqs. (2), two prominent types of connection weight matrices  $w$  have been considered:

$$w^{(A)} = \begin{pmatrix} a & -a \\ b & -b \end{pmatrix}, \quad w^{(B)} = \begin{pmatrix} \alpha & -\beta \\ \beta & \alpha \end{pmatrix}.$$

The type *A* is widely studied [12,14–16]. As shown by Wang [12], for  $u=v=0$ , the choice  $a \geq 2b$  produces a period-doubling route to chaos for varying the parameters  $\mu$  or  $\sigma$ . In the chaotic regime, two chaotic attractors may coexist with distinct attraction basins. Constant external input can switch the dynamics from one attractor to the other [14,15]. This allows us to perform simple computational tasks using chaotic attractors. In addition, the system (2) can encode information in the sense of representing stimulus intensity through changes in system dynamics [14].

The type-*B* connectivity results in a system with periodic oscillatory dynamics [19]. For  $\alpha^2 + \beta^2 > 1$ , a limit cycle attractor occurs via a secondary Hopf bifurcation (or Neimark-Sacker bifurcation) and may vanish by means of a saddle-node or limit-cycle bifurcation.

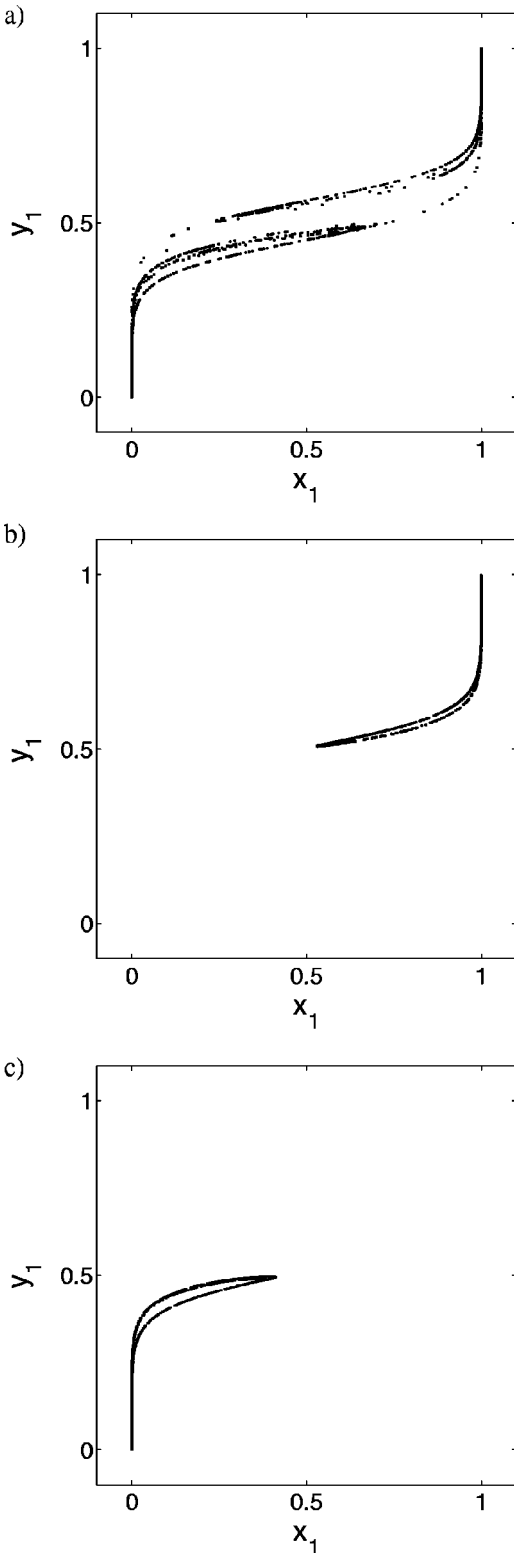


FIG. 2. Chaotic attractors corresponding to the (a) “ground,” (b) “up,” and (c) “down” states of Eq. (4).

**B. A neural oscillator with delay**

With respect to performing computational tasks, the model (2) has serious shortcomings. First, the system in its ground state has two distinct attractors. Second, the effect of

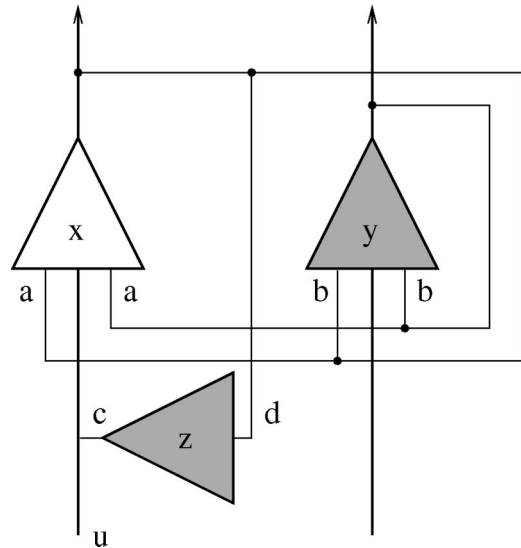


FIG. 3. Schema of the discrete-time oscillator with delayed feedback loop. Filled elements indicate inhibitory neurons.

external input is not canceled when the input is turned off, i.e., the system does not fall back to a defined ground state. Finally, the chaotic attractors are separated by an unstable fixed point, which may interfere unfavorably with the network dynamics by capturing the orbit. A modified system

$$x^{t+1} = f[ax^t - ay^t + cf(dx^{t-1}) + u], \tag{4}$$

$$y^{t+1} = f(bx^t - by^t + v),$$

was suggested to counter these defects by introducing a time-delayed feedback on the excitatory neuron [15]. This modification results in a sigmoidal-shaped chaotic attractor as a “ground state.” In response to external input, the system constrains its dynamics onto delimited parts of the attractor as long as the input is supplied. Excitatory input on neuron  $x$  confines the output of  $(x, y)$  to an attractor in the upper half of the phase space, whereas inhibitory input results in an attractor in the lower half of the phase space. In the following, we refer to these states as “ground,” “up,” and “down” states, respectively (cf. Fig. 2).

The introduction of a time-delayed feedback seems biologically unjustified. It is believed that chaos in biological networks arises from the interaction between different network areas separated by long and/or slowly conducting paths of signal transmission, effectively acting as a time-delayed feedback loop. But instead of using Eq. (4) with delayed self-coupling, a network with four neurons can be used to obtain identical dynamics. The four-neuron network can be used as a simple logical unit, capable of performing for instance, the XOR function by discriminating excitatory and inhibitory input [15,16]. The connection scheme for introducing the delayed feedback loop into the system given in Eqs. (2), incorporated as an additional neuron, is shown in Fig. 3.

### III. DYNAMICS OF A DRIVER-RESPONSE SYSTEM

A single neural oscillator effectively acts as a signal transducer, turning a nonoscillating input into a chaotic signal. This may allow us to encode the intensity of a sensory input in different degrees of complexity in behavior, ranging from periodic to chaotic dynamics. However, more realistic is a steady flow of incoming information interacting with ongoing activity in distributed networks. Thus, time-dependent input is more likely to be of relevance. Interactions of two chaotic neural oscillators (2) or (4), respectively, can be studied in a master-slave configuration with unidirectional coupling. Assuming that the inhibitory neurons  $y_i$  are local circuit neurons and only the excitatory neurons  $x_i$  can interact, this results in the equations

$$x_1^{t+1} = f[ax_1^t - ay_1^t + cf(dx_1^{t-1}) + \varepsilon x_2^t + u_1^t + \theta],$$

$$y_1^{t+1} = f(bx_1^t - by_1^t + v_1),$$

$$x_2^{t+1} = f[ax_2^t - ay_2^t + cf(dx_2^{t-1}) + u_2^t + \theta],$$

$$y_2^{t+1} = f(bx_2^t - by_2^t + v_2).$$

Here  $(x_1, y_1)$  is the response system (slave) and  $(x_2, y_2)$  the drive (master). The transfer function is given by the Fermi function (3) with steepness  $\sigma = 1$ , so that  $f(z) \in [0, 1]$ . The synaptic connection weight matrices for both oscillators are of type  $A$  and are identical:

$$w = \begin{pmatrix} 25 & -25 \\ 5 & -5 \end{pmatrix}. \quad (7)$$

Throughout the text, we use the parameter values  $c = -1.5$  and  $d = 0.5$ . The threshold, or bias,  $\theta$  was chosen identical for both excitatory neurons as  $\theta = 0.5$ . Via the bias, it is possible to control the system's overall activity level, which may be helpful in adjusting the network parameters so as to comply with the desired stabilization properties. The value of  $\theta = 0.5$  has been found suitable to keep the system in a chaotic state. The coupling strength between master and slave is given by  $\varepsilon$ . For  $\varepsilon = 0$ , the systems are decoupled and each system is chaotic depending on the external inputs, which are denoted by  $u_1$  and  $u_2$ . Effectively, constant external input  $u_1$  and the chaotic drive signal add up to a time-dependent input on the response system.

It is assumed that stimulus reception in biological systems, at onset and offset of input activity, respectively, stabilizes the system transiently onto a new attractor. One may also consider memory formation and retrieval as attractor stabilization (through neuromodulatory substances that enhance those couplings related to the attractor). Also, pattern recognition may be realized as a matching operation: the stored attractor is, loosely speaking, congruent with the present attractor induced by sensory input. Thus, of particular interest for our study is the behavior when drive and response system are in different initial attractor states and external input is applied. There are 18 different state configurations for the master-slave pair if  $\varepsilon \neq 0$ , determined by the sign of the coupling coefficient  $\varepsilon$  and the states of both os-

illators. In the following, we study in detail the situation when drive and response are in the “ground” state and the drive is settled into the “up” state by constant external input.

#### A. Dynamics with $u_i = 0$

Without external influences, i.e., with  $u_i = 0$  and  $\varepsilon = 0$ , the “ground” state corresponds to the unperturbed state for both oscillators. Here,  $(x_i, y_i)$  oscillates irregularly in the upper

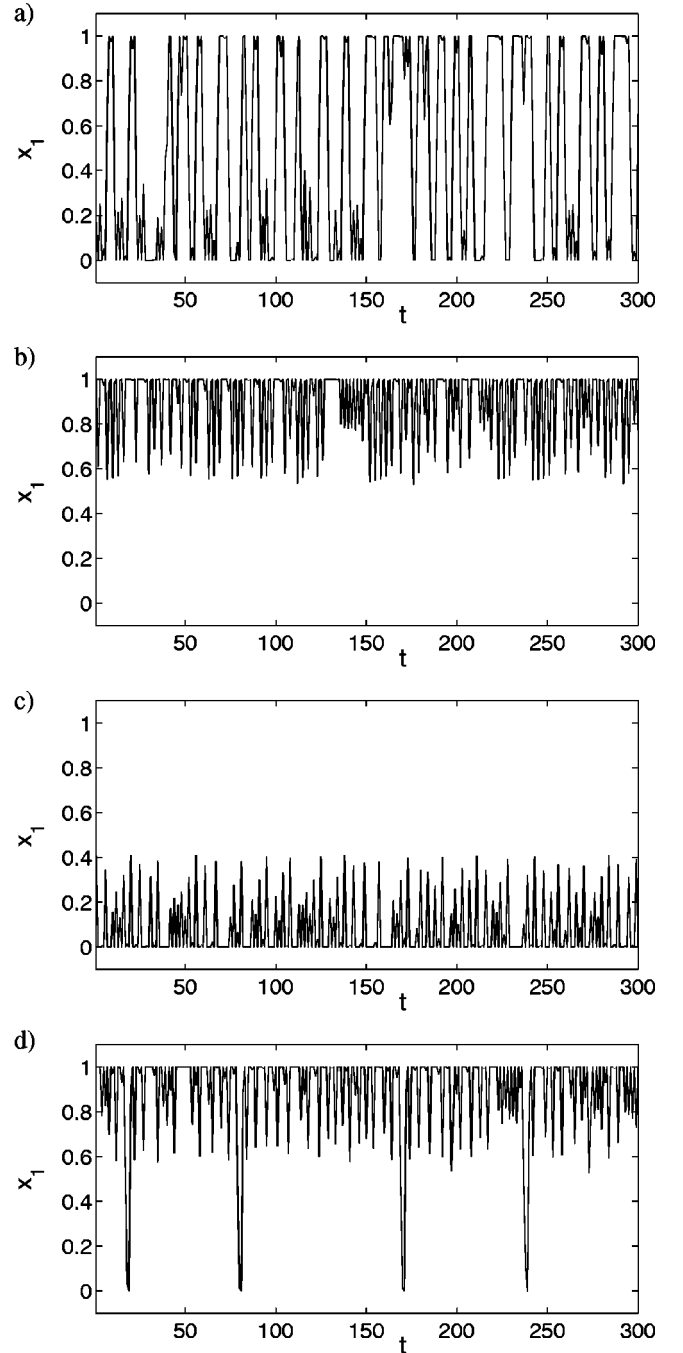


FIG. 4. Signal of neuron  $x_1$  in the “ground,” “up,” and “down” states and in the intermittent regime while adapting the “up” state.

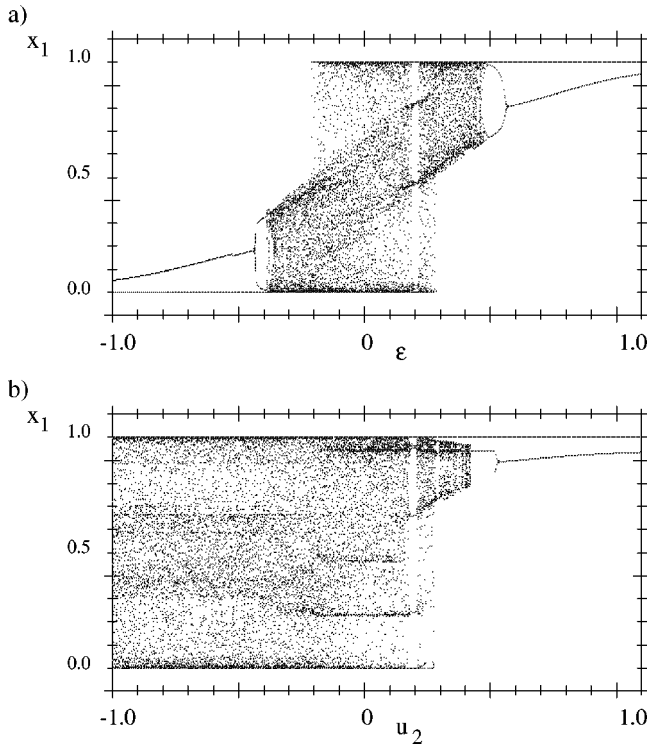


FIG. 5. Bifurcation diagrams of the output of neuron  $x_1$  (a) with external input  $u_2=1$  on  $x_2$  as a function of coupling strength  $\epsilon$ . (b) With coupling strength  $\epsilon=1$  as a function of external input  $u_2$ .

and lower halves of the phase space forming an S-shaped attractor. The effects of increasing the coupling strength  $\epsilon$  can be observed in the output signal of neuron  $x_1$  (cf. Fig. 4), in the bifurcation diagrams in Figs. 5 and 6 where the state of the excitatory response neuron  $x_1$  is plotted as a function of  $\epsilon$ , and in the phase portrait of the response oscillator (cf. Fig. 7).

When both drive and response are in the “ground” state, the chaotic driving results in an enlargement of the attractor and a chaotic response over a large range of coupling strength  $\epsilon$ . Applying weak constant external input to the drive system allows us to switch the drive from the “ground” state into the “up” or “down” state, respectively. We note that external input does not constrain to a part of the ground-state attractor in a strict mathematical sense, but we found that this new, nearby attractor appears sufficiently close (in the sense of the Hausdorff distance) to the old one.

### B. Dynamics with $u_i \neq 0$

Turning on the external input  $u_2$ , we can observe that the response system adapts to the attractor of the drive system if the coupling strength exceeds a critical value and the coupling coefficient and the input have equal signs. For  $\epsilon > 0$  and a negative input  $u_2$  to the drive, the “down” state for the drive, the response does not adapt to the attractor of the driving system. In contrast, a negative sign for the coupling strength  $\epsilon$  and positive input on the drive results in an adaptation of the response to the complementary attractor, the “down” state.

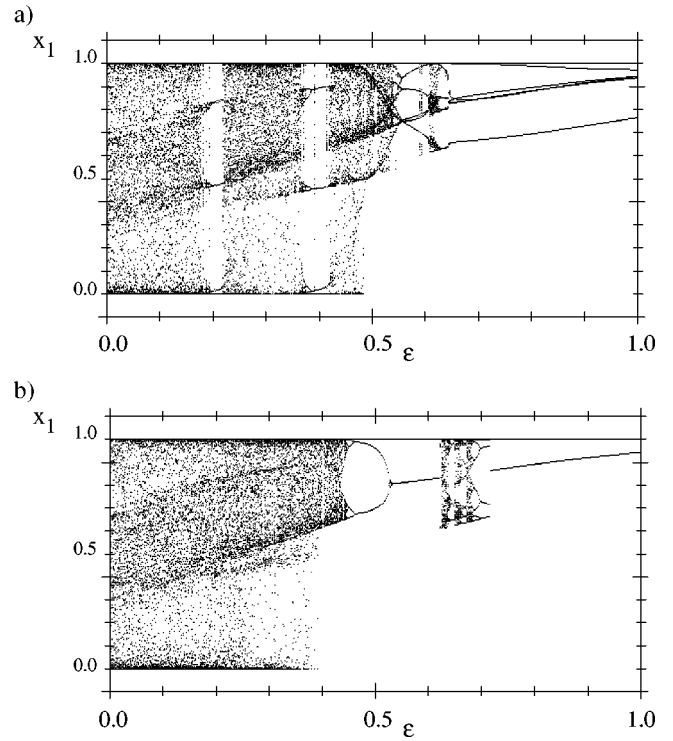


FIG. 6. Bifurcation diagram of the output of neuron  $x_1$  as a function of coupling strength  $\epsilon$  for external input strength (a)  $u_2=0.35$  and (b)  $u_2=0.45$ .

Thus, the response system is sensitive to the spatial location of the drive in phase space. The dynamics of the response restricted to the new spatial location can be either chaotic or periodic, depending on the drive strength and independent of the nature of the drive signal. Close to the critical coupling for synchronization, we can observe regimes with partial synchronization: the dynamics of the response follows the drive for short periods interrupted in irregular intervals by sudden jumps to the complementary attractor, resulting in a complex burstinglike behavior.

To estimate the parameter regions, bifurcation diagrams were evaluated using  $\epsilon$  and  $u_2$  as bifurcation parameters. To this end, one of the parameters  $\epsilon$  and  $u_2$  was kept at  $\epsilon=1$  or  $u_2=1$ , respectively, while the other parameter was varied. In general, chaotic behavior of the system (4) in response to constant external input is observed in a small parameter range between  $u_2 \approx 0.3$  and  $u_2 \approx 0.6$ . For larger values of input strength, we note that the single oscillator typically is not chaotic but oscillates periodically. Thus, we expect that chaotic behavior of the response in the “up” state can be found in a corresponding parameter regime for  $\epsilon$ . First we fixed  $\epsilon$  and obtained the output of neuron  $x_1$  as a function of external input  $u_2$  on neuron  $x_2$ . We start a detailed analysis with  $\epsilon=0.3$ . For this coupling strength, the response system switches to the “up” state if the external input strength exceeds  $u_2=0.89$ . A periodic window can be observed for  $1.064 < u_2 < 1.243$ . For larger values, the output of neuron  $x_1$  is again in the chaotic “up” state. For  $\epsilon=0.4$ , the response system jumps to the “up” state if  $u_2 > 0.39$  and remains chaotic also for larger values of input strength  $u_2$ . Further

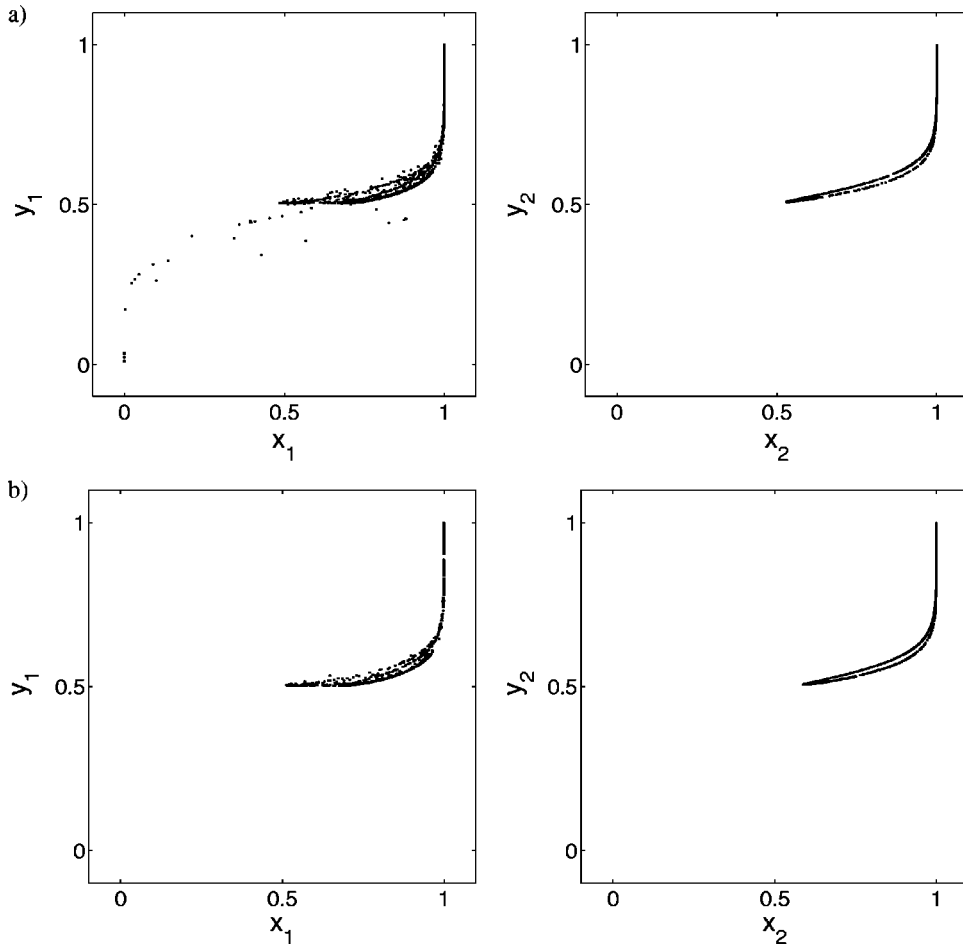


FIG. 7. Attractor of response (left) and drive (right) for  $\varepsilon=0.5$  and applied external input  $u_2 = 0.3$  (top) and  $u_2=0.37$  (bottom).

increasing  $\varepsilon$  again yields a critical value of  $u_2 \approx 0.39$  for adjusting to the “up” state, while chaotic behavior is now observed in a smaller region of  $u_2$ .

For fixed external input  $u_2$  and varied coupling strength  $\varepsilon$ , the bifurcation diagrams show qualitatively similar behavior. For  $u_2=0.35$ , periodic windows can be observed for  $\varepsilon \approx 0.2$  and  $\varepsilon \approx 0.4$ . The intermittent regime then follows, and at  $\varepsilon \approx 0.48$  the response is completely settled into the “up” state. This chaotic regime is interrupted by a small periodic window at  $\varepsilon \approx 0.51$ . At  $\varepsilon \approx 0.538$ , the chaotic attractor disappears via a reverse sequence of period doublings. At  $\varepsilon \approx 0.6$  and  $u_2=0.35$ , a new chaotic attractor appears in the “up” state region via a crisis as can be seen in Fig. 6(a).

Increasing external input strength  $u_2$  yields similar behavior, but shifts the parameter regions towards larger values. The behavior for  $u_2=0.45$  is shown in Fig. 6(b).

#### IV. GENERALIZED SYNCHRONIZATION

For coupled chaotic systems, intuition about criteria and conditions of synchronization may fail. Previous studies showed that there is no sharp synchronization threshold. Instead, there are multiple thresholds, each associated with an unstable periodic orbit. Near each synchronization threshold there can be intermittent bursting (attractor bubbling) of the system out of the synchronous state when there is a small amount of noise or parameter mismatch present [17]. The

attractor may exhibit riddled basins, so that a prediction of the synchronized state is almost impossible by just knowing initial conditions [18].

Synchronization of chaotic systems and the stability of the synchronized state can be determined by the spectrum of the Lyapunov exponents. One obtains synchronization only if the maximal Lyapunov exponent of the response subsystem is negative. For the system in Eqs. (1) one has  $d+r$  Lyapunov exponents. Of these,  $d$  exponents coincide with those of the drive and are denoted by  $\lambda_i^{(V)}$ ,  $i=1, \dots, d$ . The other  $r$  exponents  $\lambda_i^{(U)}$ ,  $i=1, \dots, r$ , are assigned to the response and are called conditional Lyapunov exponents. Ranking the Lyapunov exponents by magnitude ( $\lambda_1 > \lambda_2 > \dots$ ), one obtains generalized synchronization if  $\lambda_1^{(U)} < 0$ . The attractor dimension of the combined system  $U+V$  can be estimated with the Kaplan-Yorke formula

$$D_{U+V} = l + \sum_{j=1}^l \frac{\lambda_j}{|\lambda_{l+1}|}, \quad (8)$$

where  $l$  is defined by the conditions  $\sum_{j=1}^l \lambda_j > 0$  and  $\sum_{j=1}^{l+1} \lambda_j < 0$ . To obtain the Lyapunov exponents, we need the linearized equations. Therefore, we rewrite the time-delayed system (4) as an equivalent three-dimensional system,

$$x_i^{t+1} = f(ax_i^t - ay_i^t + cz_i^t + u_i),$$

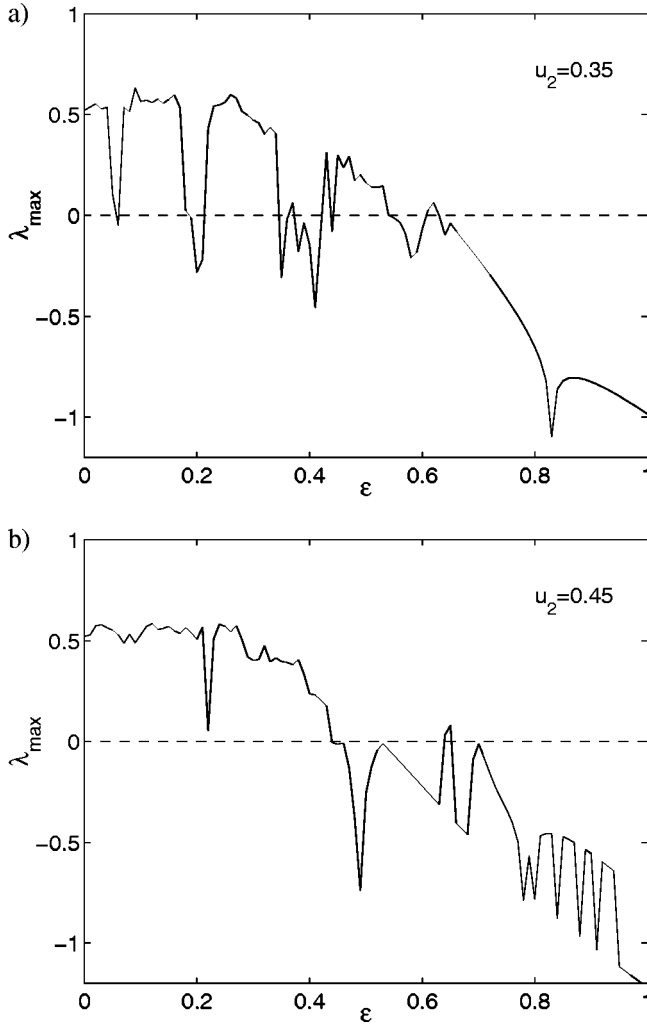


FIG. 8. Maximal Lyapunov exponent for the joint driver-response system with fixed external input (a)  $u_2=0.35$  and (b)  $u_2=0.45$  as a function of master-slave coupling strength  $\varepsilon$ .

$$\begin{aligned} y_i^{t+1} &= f(bx_i^t - by_i^t + v_i), \\ z_i^{t+1} &= f(dx_i^t), \end{aligned} \quad (9)$$

to construct the master-slave system in analogy to Eqs. (5) and (6). For this system, the Jacobian matrix can be easily determined. The spectrum of the Lyapunov exponents for the single system (9) was calculated as  $\lambda_1 \approx 0.502$ ,  $\lambda_2 \approx -2.43$ , and  $\lambda_3 \approx -8.17$  for the “ground” state ( $u_i=0$ ) and  $\lambda_1 \approx 0.427$ ,  $\lambda_2 \approx -4.334$ , and  $\lambda_3 \approx -7.145$  for the “up” state with constant external input  $u_i=0.3$ . In Fig. 8, we show the maximal conditional Lyapunov exponent of the master-slave system as a function of the coupling strength  $\varepsilon$  and different input parameters  $u_2$ . The qualitative dependence on the coupling strength  $\varepsilon$  reproduces the behavior of the oscillator as observed in the bifurcation diagrams in Fig. 6. The dimension for the joint system was calculated as  $D_{U+V}=2.03$  for  $u_2=0.35$  at  $\varepsilon=0$  and as  $D=1.3474$  at  $\varepsilon=0.49$ , where the response adapts to the “up” state.

In the parameter regimes where the response adapts to the state of the drive, the maximal Lyapunov exponent decreases

but remains positive. For a larger coupling strength  $\varepsilon$ , the maximal conditional Lyapunov exponent becomes negative, indicating generalized synchronization. For parameter values where the new chaotic attractor appears at  $\varepsilon \approx 0.6$ , the Lyapunov exponent becomes positive again. An inspection of the regions of a negative maximal Lyapunov exponent shows different behavior depending on the dynamics of the drive system. For a periodic drive, the response may also become periodic. For values of  $u_2$  yielding a chaotic drive signal, we can observe chaotic dynamics of the response on a much smaller scale, in the form of small-amplitude fluctuations (presumably due to the response operating near the saturation of the Fermi output function). It seems that the dynamical behavior of the response system is completely determined by the drive. To investigate this in more detail, we consider two identical response systems, differing only in their initial amplitudes, and driven by a common drive system. In the parameter regime where the original chaotic attractor disappears via a sequence of reverse period doublings, we can observe a time shift or a delayed synchronization between both response systems. Near the bifurcation points, the delay can be decreased. This behavior seems plausible since in this parameter regime the chaotic dynamics of the response can only be observed as small-amplitude fluctuations. Between bifurcation points, the perturbations by the chaotic drive are not sufficient to synchronize the “periodic” orbits of the response systems.

The most interesting behavior is found in parameter regimes where the maximal conditional Lyapunov exponent crosses  $\lambda_1^{(U)}=0$ , or remains close to zero. In Fig. 8, we can observe that the periodic windows in Fig. 6 coincide with the main minima of the maximal Lyapunov exponent. For example, for external input  $u_2=0.35$  there is a region  $0.35 < \varepsilon < 0.64$  of the master-slave coupling where the Lyapunov exponent changes its sign several times. At  $\varepsilon=0.35$  and  $\varepsilon=0.37$ , the response system is oscillating periodically in the “up” state or the “ground” state, respectively. For  $0.46 < \varepsilon < 0.54$ , the response system is in the chaotic “up” state. At  $\varepsilon=0.36$ ,  $\varepsilon=0.43$ , and  $\varepsilon=0.45$ , the response is in the intermittent regime where the synchronization is interrupted by sudden excursions off the “up” state.

## V. DISCUSSION

Chaotic systems are characterized by their sensitive dependence on initial conditions. Small perturbations of the chaotic system can cause large and swift responses. This greatly improves the flexibility of a system to be used in various applications. Coupled chaotic maps have been proposed as a basis of high-tech sensors or secure communication devices [20]. In addition, it was shown that weakly connected mappings with chaotic dynamics have neurocomputational properties [21].

A single system (9) is capable of spatiotemporal information processing. External, chaotic input from an identical system induces a variety of dynamic behaviors in response to the chaotic drive. Possibly the response system adjusts its state to the state of the driving oscillator. Our results show that the response system is more sensitive to the spatial lo-

cation (corresponding to the “up” or “down” states, respectively) of an external driving than to the nature of the input (constant, periodic, or chaotic). Thus the master-slave system (9) may provide an example of a chaotic system that can generate spatiotemporal correlations by adapting to a state of the drive, accompanied by either synchronization or temporally uncorrelated activity. The state of the response is a function of the drive, depending on the restrictions imposed by the strength of the master-slave coupling and the strength of external input to the drive. Varying external input  $u_2$  may yield chaotic as well as periodic activity of the drive. If the master-slave coupling exceeds a critical value, the response follows the drive, independent of the nature of the driving signal. The Lyapunov exponents shown in Fig. 8 confirm the conclusions drawn from the bifurcation diagrams in Figs. 5 and 6. If both systems are set into the chaotic “up” state, the maximal Lyapunov exponent corresponding to the response system first remains positive for intermediate coupling strength and then for larger coupling strength a negative maximal Lyapunov exponent is observed, i.e., generalized synchronization.

In the parameter regime where the response system adapts to the state of the drive, we can also observe intermittent behavior or partial synchronization. The dynamics of the response follows the drive for longer periods. This is interrupted by sudden jumps to the complementary attractor and results in complex burstinglike behavior. Such behavior has been found in several coupled chaotic systems and is referred to as on-off intermittency [17]. This kind of intermittency is characterized by short periods of desynchronization interrupting the synchronized activity. The origin of these short events of desynchronization is unstable periodic orbits (UPOs) of the drive attractor that fail to entrain the corresponding fixed point or periodic orbit of the response system. When driven with one of these UPOs, the response system does not synchronize, but oscillates in a way different from the drive. In the joint space of drive and response, these UPOs are transversally unstable, i.e., in their vicinity the synchronization manifold is repelling, not attracting. Whenever an almost synchronized trajectory comes close to a transversally unstable UPO, it is repelled from the synchronization manifold and synchronization breaks down for a short period of time.

There is ample experimental evidence for chaotic behavior in single neurons and on the network level. The biological relevance of the model (2) with type A connectivity is discussed in detail elsewhere [14]. Of course our model (4) is also a simplified analogy of a real biological system. Thus, it has several limitations and there is no guarantee that the behavior of the model is actually relevant for biological systems. However, studies of complex oscillator ensembles must proceed from simplified and therefore somewhat unrealistic models. We are only beginning to understand the brain as an ensemble of neuronal oscillators instead of a network of simple inhibitory and excitatory integrate-and-fire elements. There is good experimental evidence that the precise temporal pattern of neuronal activity is crucial for information processing and that studies of coupled nonlinear oscillators will lead the way to understand information pro-

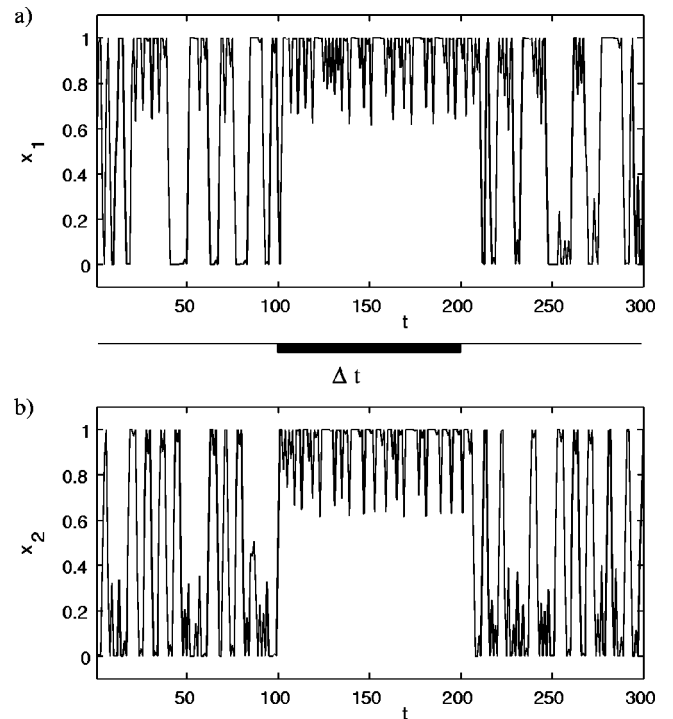


FIG. 9. Signal of the response  $x_1$  and the drive  $x_2$  for a “pulsed” input  $u_2$  on the drive starting at  $t=100$  for  $\Delta t=100$  iterations.

cessing in the brain. One firm argument in favor of such an approach is the coexistence of reciprocal as well as master-slave coupling in the nervous system along with the finding that these connections serve functions, e.g., in stimulus recognition, which cannot be explained by ascribing to them just feedback-control such as in a flow-limiting control device. Nevertheless, there are numerous instances of master-slave systems in biology that inspired the investigations presented here.

Networks of coupled units showing regular, periodic dynamics are widely studied in the neurobiological context; only a few studies on synchronization phenomena focus on the behavior of coupled chaotic subsystems [22]. Coupled chaotic systems provide the advantage, like real biological networks, that synchronization is sensitive to changes in coupling strength. This may enable that transitions from synchronization to desynchronization and vice versa can be modulated by changes in synaptic coupling strength. In our system, see Fig. 9, we can observe that, when a pulsed input  $u_2$  is applied on the drive, the adaptation of the response system to the state of the drive occurs instantaneously. In contrast, the rate of convergence to the attractors, under appropriate values of coupling strength, is very slow for regular, periodic oscillators.

Of particular interest are also the relations between discrete and continuous systems. Discrete-time systems also arise in iterations of Poincaré or time- $T$  maps of continuous flows. When such a mapping has a fixed point, the corresponding flow has a limit cycle solution. When, for example, the mapping undergoes a saddle-node bifurcation, then there is also a bifurcation in the flow: a stable and an unstable limit



cycle coalesce and disappear. Weakly connected mappings near fixed points or limit cycles have been studied by Hoppensteadt and Izhikevich [23]. They found an intimate relationship between canonical models for mappings and flows. Thus, we expect to observe similar properties in the discrete-time oscillator of type-*B* connectivity as found in the networks of continuous-time bistable oscillators studied in [24]. This, however, will be the subject of further studies.

## ACKNOWLEDGMENTS

J.S. wants to thank Professor Peter Grassberger for his kind hospitality at the John-von-Neuman Institut for Computing at the FZ Jülich, where parts of the calculations were carried out. The authors would like to thank Rodrigo Quiñero and Peter Ashwin for fruitful discussions and the reading of a first draft of this manuscript.

- 
- [1] A. Babloyantz and C. Lourenco, Proc. Natl. Acad. Sci. U.S.A. **91**, 9027 (1990).
  - [2] I. Tsuda, Neural Networks **5**, 313 (1992); M. Kushibe, Y. Liu, and J. Ohtsubo, Phys. Rev. E **53**, 4502 (1996).
  - [3] P.F.M.J. Verschure, Complex Syst. **5**, 359 (1991).
  - [4] A. Priel and I. Kanter, Phys. Rev. E **59**, 3368 (1999).
  - [5] W.J. Freeman, Biol. Cybern. **56**, 139 (1987); C.A. Skarda and W.J. Freeman, Behav. Brain Sci. **10**, 161 (1987); Y. Yao and W.J. Freeman, Neural Networks **3**, 153 (1990); H.-J. Chang and W.J. Freeman, *ibid.* **9**, 1 (1996).
  - [6] D. Terman and D. Wang, Physica D **81**, 148 (1995); D. Hansel, G. Mato, and C. Meunier, Neural Comput. **7**, 307 (1995); P. Bush and T.J. Sejnowski, J. Comput. Neurosci. **3**, 91 (1996).
  - [7] L.M. Pecora and L. Carroll, Phys. Rev. Lett. **64**, 821 (1990).
  - [8] L.M. Pecora and L. Carroll, Phys. Rev. A **44**, 2374 (1991).
  - [9] N.F. Rulkov, M.M. Sushchik, L.S. Tsimring, and H.D.I. Abarbanel, Phys. Rev. E **51**, 980 (1995).
  - [10] K. Pyragas, Phys. Rev. E **54**, 4508 (1996).
  - [11] J. Arnhold, P. Grassberger, K. Lehnertz, and C.E. Elger, Physica D **134**, 419 (1999); R. Quiñero, J. Arnhold, and P. Grassberger, Phys. Rev. E **61**, 5142 (2000).
  - [12] X. Wang, Complex Syst. **5**, 425 (1991).
  - [13] H.R. Wilson and J.D. Cowan, Biophys. J. **12**, 1 (1972).
  - [14] A.A. Minai and T. Anand, Phys. Rev. E **57**, 1559 (1998).
  - [15] A. Klotz and K. Bräuer, Neural Networks **12**, 601 (1999).
  - [16] J. Schwarz, A. Klotz, K. Bräuer, A. Stevens, and M. Bartels, in *Proceedings of the 2nd ICSC Symposium Neural Computation*, edited by H. Bothe and R. Rojas (ICSC Academic Press, Millet, Canada, 2000), pp. 392–398.
  - [17] P. Ashwin, J. Buescu, and I. Stewart, Phys. Lett. A **193**, 126 (1994).
  - [18] J.C. Alexander, J.A. Yorke, Z. You, and I. Kan, Int. J. Bifurcation Chaos Appl. Sci. Eng. **2**, 795 (1992); J.F. Heagy, T.L. Carroll, and L. Pecora, Phys. Rev. Lett. **73**, 3528 (1994).
  - [19] A. Tonnelier, S. Meignier, H. Bosch, and J. Demongeot, Neural Networks **12**, 1213 (1999).
  - [20] C. Zhou and C.-H. Lai, Phys. Rev. E **59**, 4007 (1999).
  - [21] K. Kaneko, Physica D **77**, 456 (1994); A.S. Pitkovski and J. Kurths, *ibid.* **76**, 411 (1994).
  - [22] F. Pasemann and T. Wennekers, Network Comput. Neural Syst. **11**, 41 (2000).
  - [23] F.C. Hoppensteadt and E.M. Izhikevich, *Weakly Connected Neural Networks* (Springer, Berlin, 1997).
  - [24] J. Schwarz, A. Sieck, G. Dangelmayr, and A. Stevens, Biol. Cybern. **82**, 231 (2000); J. Schwarz, K. Bräuer, G. Dangelmayr, and A. Stevens, J. Phys. A **33**, 3555 (2000).